

Journal Pre-proof

Discovery of bardoxolone derivatives as novel orally active necroptosis inhibitors

Yuanyuan Wang, Hao Ma, Jiaxuan Huang, Zhengguang Yao, Jianqiang Yu, Wannian Zhang, Lichao Zhang, Zhibin Wang, Chunlin Zhuang



PII: S0223-5234(20)31002-3

DOI: <https://doi.org/10.1016/j.ejmech.2020.113030>

Reference: EJMECH 113030

To appear in: *European Journal of Medicinal Chemistry*

Received Date: 4 September 2020

Revised Date: 15 November 2020

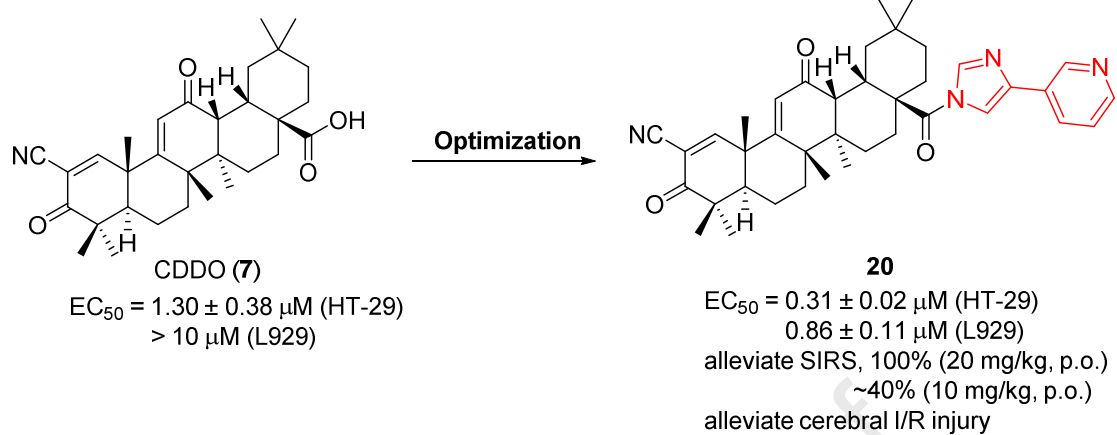
Accepted Date: 15 November 2020

Please cite this article as: Y. Wang, H. Ma, J. Huang, Z. Yao, J. Yu, W. Zhang, L. Zhang, Z. Wang, C. Zhuang, Discovery of bardoxolone derivatives as novel orally active necroptosis inhibitors, *European Journal of Medicinal Chemistry*, <https://doi.org/10.1016/j.ejmech.2020.113030>.

This is a PDF file of an article that has undergone enhancements after acceptance, such as the addition of a cover page and metadata, and formatting for readability, but it is not yet the definitive version of record. This version will undergo additional copyediting, typesetting and review before it is published in its final form, but we are providing this version to give early visibility of the article. Please note that, during the production process, errors may be discovered which could affect the content, and all legal disclaimers that apply to the journal pertain.

© 2020 Elsevier Masson SAS. All rights reserved.

Graphical Abstract



Discovery of bardoxolone derivatives as novel orally active necroptosis inhibitors

Yuanyuan Wang^{†§,1}, Hao Ma^{†J,1}, Jiaxuan Huang^{†¶,1}, Zhengguang Yao,[†] Jianqiang Yu[¶], Wannian Zhang^{†¶},
Lichao Zhang,^{§,*} Zhibin Wang^{†*}, Chunlin Zhuang^{†¶*}

[†] School of Pharmacy, Second Military Medical University, 325 Guohe Road, Shanghai 200433, China

[¶] School of Pharmacy, Ningxia Medical University, 1160 Shengli Street, Yinchuan 750004, China

^J Chinese Academy of Medical Sciences and Peking Union Medical College, 2A Nan Wei Road, Beijing 100050, China

[§] Department of Pharmacy, Shanghai Municipal Hospital of Traditional Chinese Medicine, 274 Middle Zhijiang Road, Shanghai 200071, China

Supporting Information

AUTHOR INFORMATION

Corresponding Author

* E-mail: zclnathan@163.com (Chunlin Zhuang), methyl@smmu.edu.cn (Zhibin Wang), chang-haiskin@163.com (Lichao Zhang)

Author Contributions

¹ These authors contributed equally to this work.

Notes

The authors declare no competing financial interests.

ABSTRACT

Necroptosis is a form of programmed cell death that contributes to the pathophysiology of cerebral ischemia/reperfusion (I/R) injury. In this study, bardoxolone (CDDO, **7**) was an inhibitor of necroptosis identified from an in-house natural product library. Further optimization led to identify a more potent analogue **20**. Compound **20** could effectively protect against necroptosis in human and mouse cells. The antinecrototic effect could also be synergized with other necroptosis inhibitors. It blocked necrosome formation by targeting Hsp90 to inhibit the phosphorylation of RIPK1 and RIPK3 in necroptotic cells. In vivo, this compound was orally active to alleviate TNF-induced systemic inflammatory response syndrome (SIRS) and cerebral I/R injury. Our results suggested that **20** could be a lead compound for discovering necroptosis inhibitors in I/R treatment.

■ INTRODUCTION

Programmed cell death (PCD) has been recognized to mediate normal tissue homeostasis and closely relate with multiple human diseases.[1] Caspase-dependent apoptosis was the first well-characterized and was recognized as the only form of PCD in a long period of time.[2, 3] Oppositely, necrosis was traditionally considered as an uncontrolled accidental cell death (ACD) triggered by physical stresses in a totally different manner.[4, 5] In the last 30 years, more and more evidences have supported that a subset of necrosis is an important form of PCD, which has been first named as “necroptosis” by Yuan et al.[6] Necroptosis is now defined as a caspase-independent PCD that plays a critical role in various lethal diseases such as ischemia-reperfusion injury, systemic inflammatory response syndrome (SIRS), atherosclerosis, etc.[6-9] Thus, targeting the pathologic necroptosis pathway has been deemed as a novel strategy for treating these diseases.[7]

Necroptosis is triggered by the activation of death receptors and tumor necrosis factor- α (TNF- α) is best understood to activate the receptor.[10] In response to the activation, downstream receptor-interacting protein kinase 1 (RIPK1) is recruited and activated to interact with RIPK3 to initiate the formation of necrosomes and mediate the recruitment and phosphorylation of mixed lineage kinase domain-like protein (MLKL).[11-14] Oligomers are formed from phosphorylated MLKL, which is then translocated into the plasma membrane to trigger membrane rupture to mediate necrotic cell death.[15-18] Necroptosis is considered to be mediated by RIPK1, RIPK3, and MLKL, which have been identified as critical therapeutic targets.[19]

In 2005, a pioneering work by Yuan group reported the first necroptosis inhibitor Nec-1,[6] and to date more than 20 classes of inhibitors have been identified.[20] Compound **1**, named GSK2982772 (**Figure 1**), possessing highly RIPK1 selective inhibitory activity, has been advanced into phase II trials in several indications including ulcerative colitis (UC) (NCT02903966), psoriasis (NCT02776033) and rheumatoid arthritis (NCT02858492).[21-24] An analogue **2**, named GSK3145095, has been advanced to phase I/II trials in subjects with pancreatic ductal adenocarcinoma cancer (PDAC) and other tumors (NCT03681951).[25] DNL747 is a RIPK1 inhibitor with undisclosed chemical structure, has been ad-

vanced into phase I trials to evaluate the safety, tolerability, PK, and PD in patients with amyotrophic lateral sclerosis (ALS, NCT03757351) and Alzheimer's disease (AD, NCT03757325).[26, 27] Natural products, with strong biocompatibility, have been the most successful source of potential drug leads.[28] A noncanonical Hsp90 inhibitor **3**, covalently modifying Cys420 of Hsp90 was reported to block RIPK3-dependent necroptosis in HT-29 cells ($IC_{50} = 200$ nM).[29] Compound **4**, named 6E11, selectively targeting RIPK1 ($K_D = 130$ nM), exhibited anti-necroptosis in Jurkat T cells.[30] Compounds **5-6**, named geldanamycins, were reported to decrease RIPK1 and Hsp90 proteins, protecting against neuronal injury.[31]

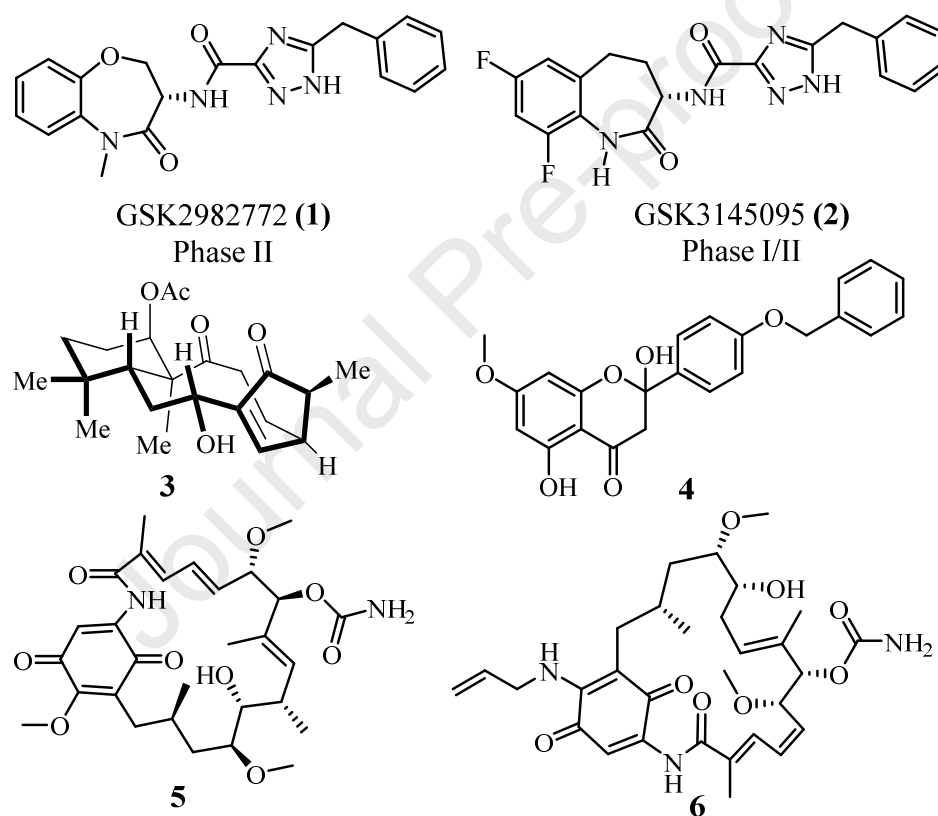


Figure 1. Disclosed necroptosis inhibitors in the clinical trials and inhibitors from natural sources

Thus, novel chemical structures with valuable biological activities and specificities may be further provided by analyzing other natural sources. In this study, we found that natural product oleanolic acid derivative, 2-cyano-3,12-dioxooleana-1,9(11)-dien-28-oic acid (CDDO, **7**) was a novel inhibitor of

necroptosis. Furthermore, highly potent analogues were developed based on the CDDO template and the in vivo efficacy was also evaluated.

■ RESULTS AND DISCUSSION

Drug screening identifies CDDO as a necroptosis inhibitor. An in-house library of ~300 natural products and nature-like derivatives was established and screened for their ability to block TNF α -induced necroptosis. HT-29 cells were treated with TNF α , a Smac mimetic (SM-164), and a caspase inhibitor z-VAD-fmk (TSZ) to induce necroptosis and the cell survival ability was measured by a chemiluminescence assay for each compound at a concentration of 10 μ M (**Figure 2A**). [32, 33] Among the natural products investigated, a triterpenoid compound bardoxolone, also named CDDO, was found to clearly protect HT-29 cells from TSZ-induced necroptosis (viability > 100%, **Figure 2B**). In addition, a known inhibitor pazopanib was included as positive control, [34, 35] and was identified (viability > 80%) in our screening, supporting the validity of our experimental protocol. Phase contrast microscopy further revealed that CDDO prevented TSZ-induced necrotic morphology, including cell swelling and plasma membrane rupture (**Figure 2C**).

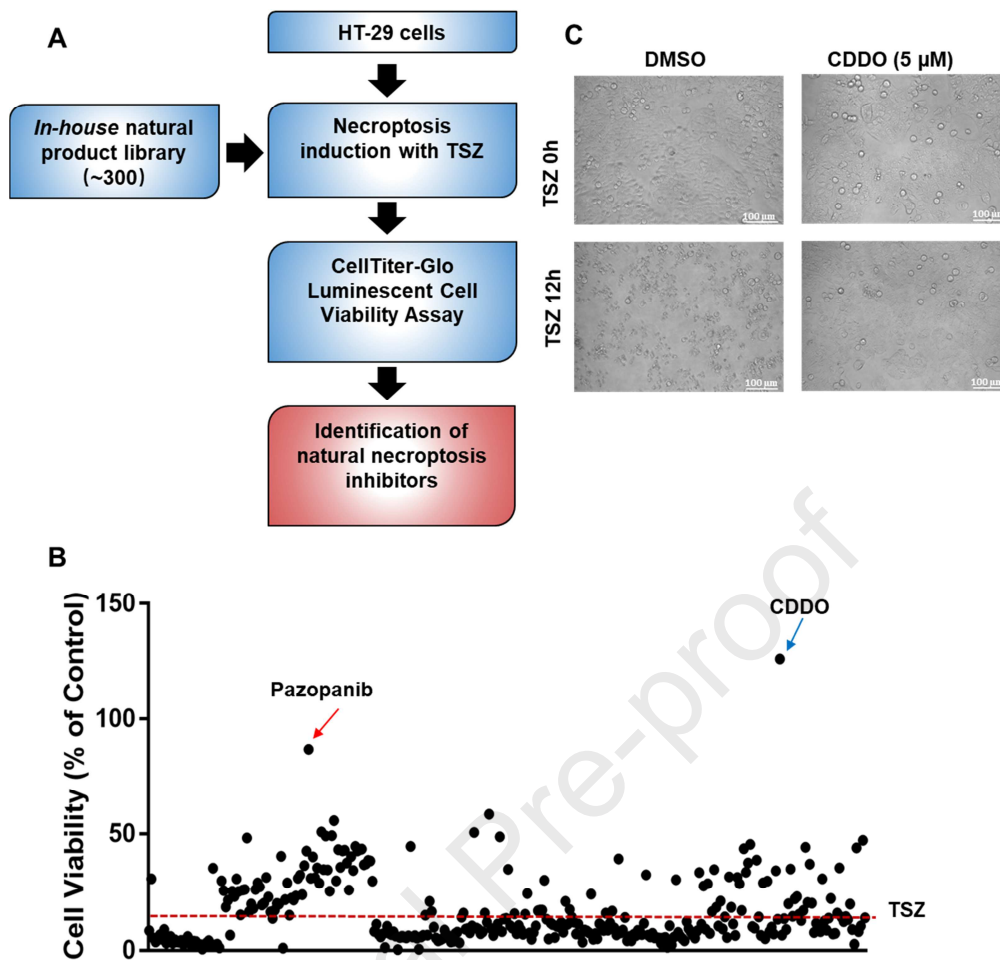


Figure 2. Identification of CDDO as a potent natural necroptosis inhibitor. (A) Schematic overview of drug screen workflow; (B) Identification of necroptosis inhibitor by cellular screening with an *in-house* natural product library. HT-29 cells were pre-treated with each compound (10 μ M) for 30 min and then stimulated with TSZ for 16 h to induce necroptosis. Cell survival was determined by a CellTiter-Glo luminescent cell viability assay and normalized to untreated control cells. (C) Representative images (200 \times) of HT-29 cells pretreated with DMSO or CDDO (5 μ M) followed by stimulation with TSZ for 12 h.

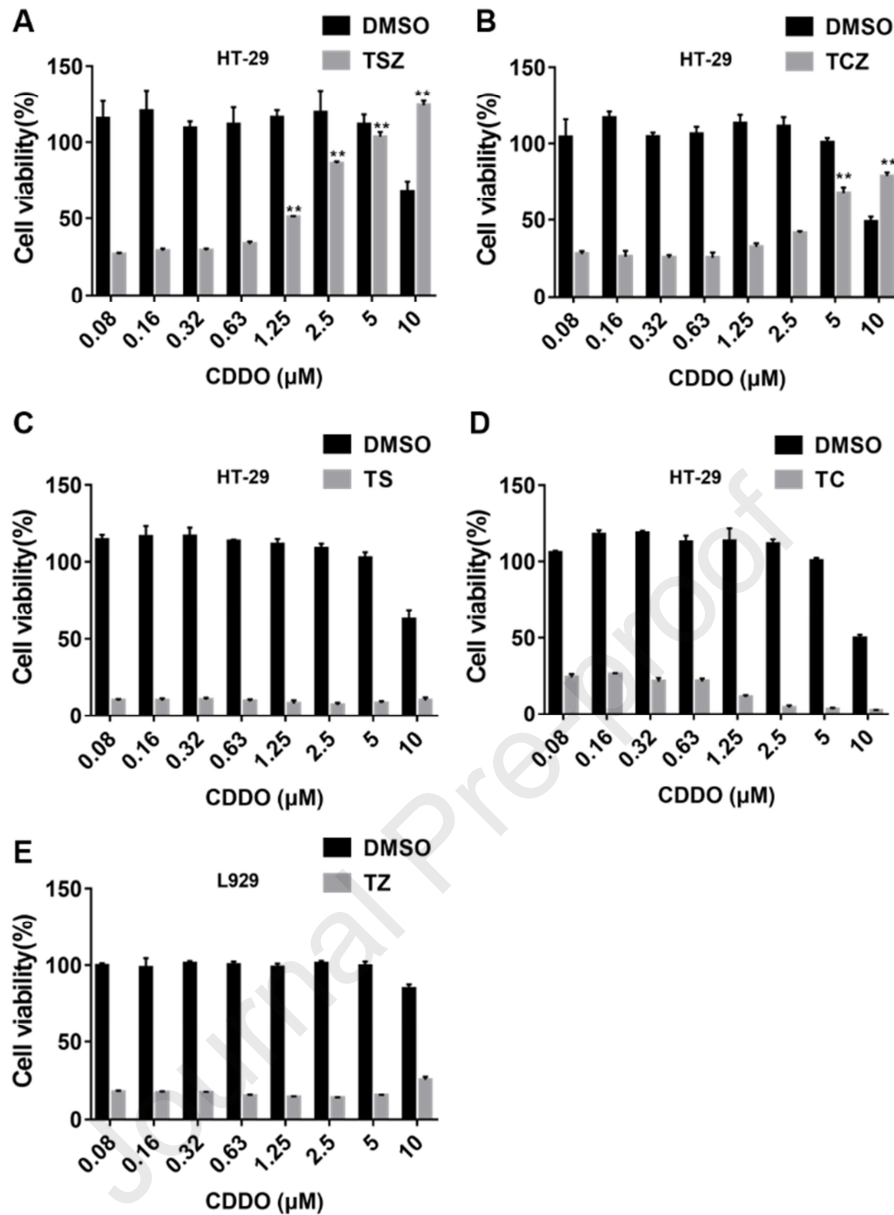


Figure 3. (A) HT-29 cells were treated with CDDO as indicated concentrations followed by stimulation with TSZ for 12 h. (B) HT-29 cells were treated with various concentrations of CDDO as indicated by stimulation with TNF- α (20 ng/mL), cycloheximide (5 μ g/mL), and z-VAD-fmk (20 μ M) (TCZ) for 16 h. (C) HT-29 cells were treated with CDDO as indicated concentrations followed by stimulation with TS for 20 h. (D) HT-29 cells were treated with various concentrations of CDDO as indicated by stimulation with TC for 24 h. (E) L929 cells were pretreated with CDDO as indicated concentrations followed by stimulation with TZ for 12 h. Results shown are means \pm S.D. from three independent experiments.

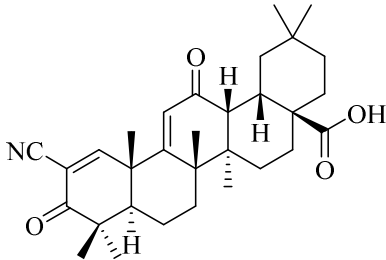
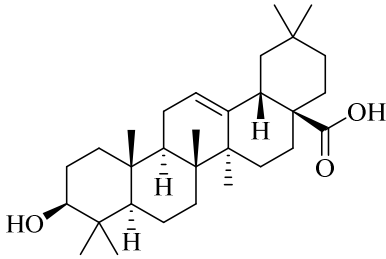
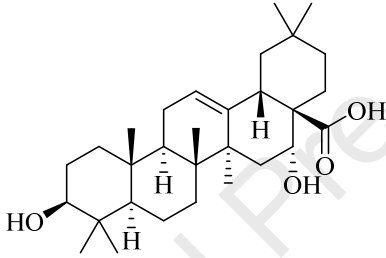
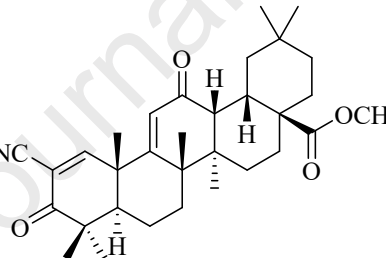
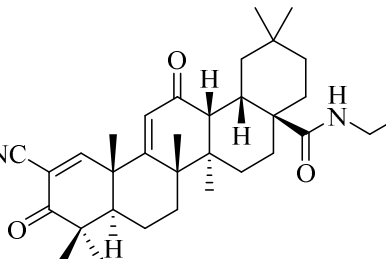
(* $p < 0.05$, ** $p < 0.01$, *** $p < 0.001$ versus TSZ, TCZ, TS, TC or TZ simulation without CDDO treatment).

We then performed a dose-response assay to quantitatively analyze the inhibitory potency of CDDO. It could dose-dependently inhibit TSZ (**Figure 3A**) with an EC_{50} value of $1.30 \pm 0.38 \mu\text{M}$ (Table 1) or TNF- α , cycloheximide, and z-VAD-FMK (TCZ)-induced necroptosis (**Figure 3B**). However, it showed cytotoxicity at $10 \mu\text{M}$. [36, 37] Remarkably, CDDO did not protect cells from TNF- α plus Smac mimetic (TS) or cycloheximide (TC)-induced apoptosis in HT-29 cells, suggesting that CDDO specifically inhibited the necroptosis pathway (**Figure 3C, D**). In murine L929 cells, we found that CDDO did not protect against necroptosis induced by TNF- α and z-VAD-fmk (TZ) (**Figure 3E**).

Identification of CDDO derivatives as potent antinecrotic agents. Structurally, CDDO is an oleanolic acid triterpenoid. Two triterpenoids, Oleanolic acid and Echinocystic acid, showed no apparent protective effect against necroptosis in human HT-29 cells at $10 \mu\text{M}$ (**Table 1**). Then, we obtained four analogues of CDDO with different substituents at the carboxyl group. CDDO-Me with a methyl ester had a lower antinecrotic effect than that of CDDO with an EC_{50} of $4.34 \pm 1.00 \mu\text{M}$ (HT-29). Similarly, it still had no effect in murine L929 cell as CDDO. The ethyl amide analogue (CDDO-EA) had a comparable EC_{50} of $1.38 \pm 0.10 \mu\text{M}$ to CDDO in HT-29 cells and an EC_{50} of $4.15 \pm 0.35 \mu\text{M}$ in L929 cells. RTA-408 with a transpositioned amide and difluoro-substitution possessed a similar inhibitory effect (HT-29, $EC_{50} = 1.41 \pm 0.16 \mu\text{M}$; L929, $EC_{50} = 5.25 \pm 0.56 \mu\text{M}$) to that of CDDO-EA.

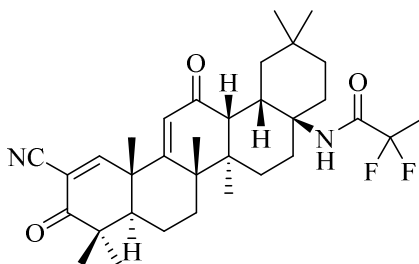
Table 1. Antinecrotic activity of commercial CDDO derivatives

Entry	Compound name	Chemical structure	HT-29, EC_{50} (μM)	L929, EC_{50} (μM)
			a	b

7	CDDO		1.30 ± 0.38	>10
8	Oleanolic acid		> 10	N.D.
9	Echinocystic acid		> 10	N.D.
10	CDDO-Me		4.34 ± 1.00	>10
11	CDDO-EA		1.38 ± 0.10	4.15 ± 0.35

12

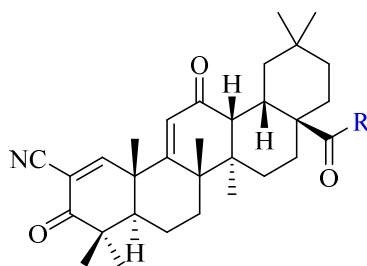
RTA-408

 1.41 ± 0.16 5.25 ± 0.56

^aHuman HT-29 cells were pretreated with DMSO or the test compound and then stimulated with TNF- α (20 ng/mL), Smac mimetic (10 nM), and z-VAD-fmk (20 μ M) (TSZ) for 16 h. The inhibition of TSZ-induced necroptosis in HT-29 cells is presented as the EC₅₀ \pm standard deviation (SD). ^bL929 cells were pretreated with DMSO or the test compound and then stimulated with mouse TNF- α (20 ng/mL) and z-VAD-fmk (20 μ M) (TZ) for 4 h. The inhibition of TZ-induced necroptosis in L929 cells is presented as the EC₅₀ \pm standard deviation (SD). All experiments were repeated independently at least three times.

Next, we synthesized some analogues based on the CDDO triterpenoid (**Table 2**). Considering the result of Table 1, the amide showed good antinecrotic activity in both human and murine cells. The benzyl amide (**13**) was evaluated to show EC₅₀ values of 1.63 ± 0.10 μ M (HT-29) and 1.03 ± 0.01 μ M (L929). Compound **14** with aliphatic amine had a less potency against necroptosis. Compound **15** with a cyclohexane group had an EC₅₀ value of 1.30 ± 0.38 μ M in human HT-29 cells, however, no apparent protective effect in murine L929 cells at 10 μ M. Then, a tetrahydronaphthalen-1-amino group (**16-17**) improved the antinecrotic activity in murine L929 cells with the EC₅₀ values lower than 1 μ M and the activity toward human HT-29 cells was kept. The chirality showed no remarkable influence on the activity. Finally, we evaluate a commercially available imidazole CDDO derivative (CDDO-Im, **18**). This compound showed the protective activity at a similar level compared with those of **13-17**. Then, if 2-pyridinyl (**19**) or 3-pyridinyl (**20**) group was attached on the imidazole, the antinecrotic activity was improved in about 7-fold in HT-29 cells and good protective activity was demonstrated toward L929 cells.

Table 2. Antinecrotic activity of amide substituted CDDO derivatives



Entry	R	HT-29, EC ₅₀ (μM) ^a	L929, EC ₅₀ (μM) ^b
13		1.63 ± 0.10	1.03 ± 0.01
14	NHCH ₂ CH ₂ NHBoc	2.81 ± 0.09	1.48 ± 0.03
15		1.30 ± 0.38	>10
16		1.91 ± 0.20	0.82 ± 0.03
17		1.81 ± 0.05	0.62 ± 0.01
18		2.10 ± 0.10	1.46 ± 0.08
19		0.29 ± 0.01	0.61 ± 0.02
20		0.31 ± 0.02	0.86 ± 0.11

^aHuman HT-29 cells were pretreated with DMSO or the test compound and then stimulated with TNF- α (20 ng/mL), Smac mimetic (10 nM), and z-VAD-fmk (20 μ M) (TSZ) for 16 h. The inhibition of TSZ-induced necroptosis in HT-29 cells is presented as the EC₅₀ \pm standard deviation (SD). ^b L929 cells were pretreated with DMSO or the test compound and then stimulated with mouse TNF- α (20 ng/mL) and z-

VAD-fmk (20 μ M) (TZ) for 4 h. The inhibition of TZ-induced necroptosis in L929 cells is presented as the $EC_{50} \pm$ standard deviation (SD). All experiments were repeated independently at least three times.

Compound 20 inhibit necroptosis and apoptosis. Compounds **19** and **20** showed the best activity at a similar level. We next randomly selected **20** for further evaluation. It efficiently restored cell viability from TSZ or TCZ -induced necroptosis in a dose-response manner (**Figure 4A, B**). The necroptotic cells could be protected completely at 0.5 and 1 μ M. Different from CDDO, this compound could protect cells from TS or TC-induced apoptosis in HT-29 cells, suggesting that compound **20** inhibits necroptosis and apoptosis pathways (**Figure 4C, D**). For murine L929 cells, it dose-dependently protected against necroptosis induced by TZ (**Figure 4E**). Thus, our results suggest that compound **20** is an effective programmed cell death inhibitor better than the parent compound CDDO.

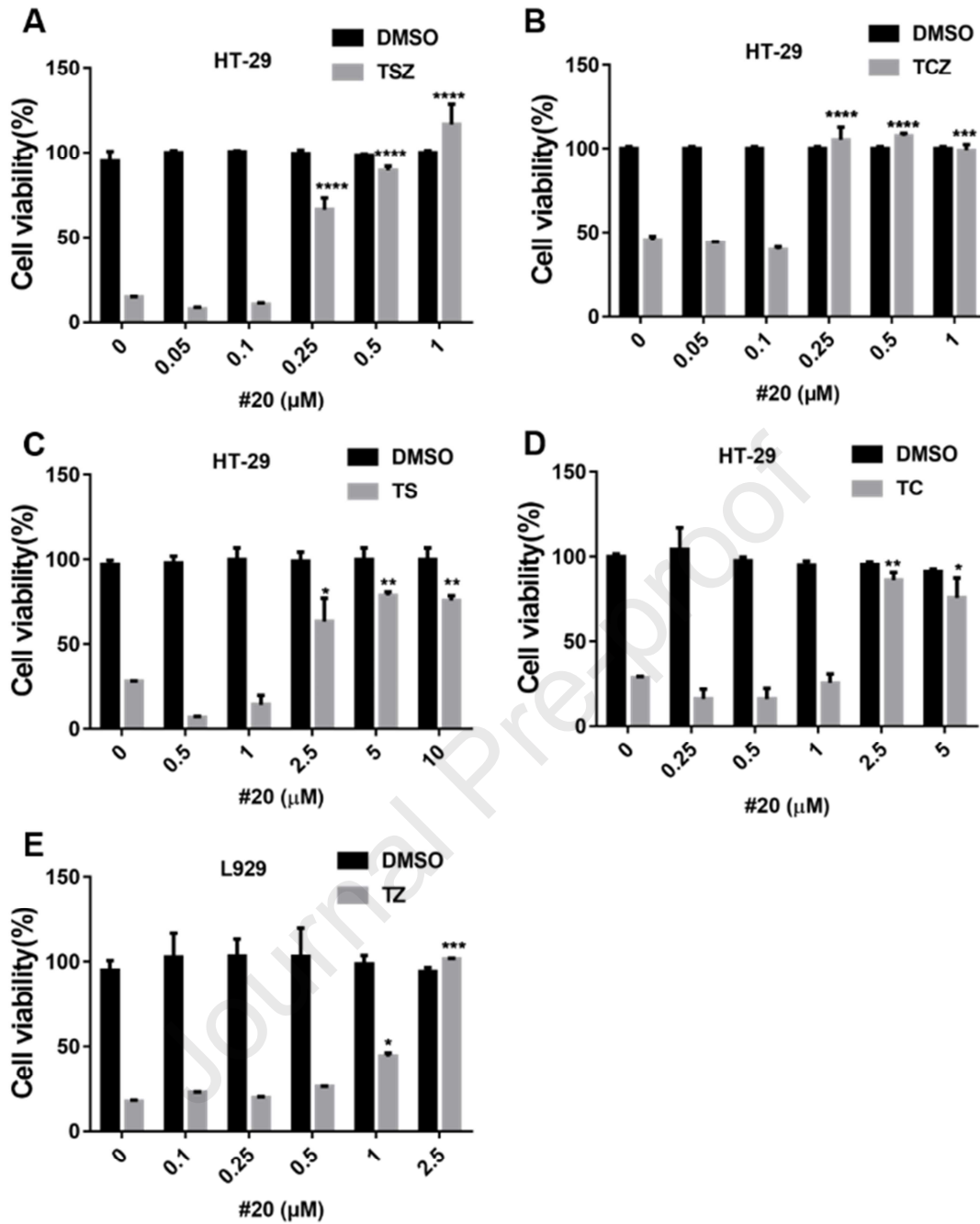


Figure 4. (A) HT-29 cells were treated with **20** as indicated concentrations followed by stimulation with TSZ for 12 h. (B) HT-29 cells were treated with various concentrations of **20** as indicated by stimulation with TNF- α (20 ng/mL), cycloheximide (5 $\mu\text{g/mL}$), and z-VAD-fmk (20 μM) (TCZ) for 16 h. (C) HT-29 cells were treated with **20** as indicated concentrations followed by stimulation with TS for 20 h. (D) HT-29 cells were treated with various concentrations of **20** as indicated by stimulation with TC for 24 h. (E) L929 cells were pretreated with **20** as indicated concentrations followed by stimulation with TZ for

12 h. Results shown are means \pm S.D. from three independent experiments. (* $p < 0.05$, ** $p < 0.01$, *** $p < 0.001$ versus TSZ, TCZ, TS, TC or TZ simulation without treatment).

Compound 20 targets Hsp90 not Nrf2 to blocks necrosome formation by inhibiting the phosphorylation of RIPK1 and RIPK3. CDDO has been reported to target multiple proteins, and Keap1-Nrf2 and Hsp90 are in the majority.[38] The representative inhibitors of these two targets have been selected to evaluate the relevance of these targets in necroptosis. However, the two Nrf2 modulators brusatol[39] and dimethyl fumarate[40] showed no protection against necroptosis at 10 μ M (**Figure 5A**). The result, suggesting that Nrf2 was not the common target for CDDO's antinecrotic effect, was consistent with the Yuan's report, which revealed the protection of necroptosis by CDDO in HT-29 cells with Nrf2 knockdown.[41] Hsp90 was reported to be associated with RIPK1[42, 43] and the necroptosis could be effectively blocked by knockdown of Hsp90.[41] Two synthetic chemical Hsp90 inhibitors (Onalespib[44] and Tanespimycin[45]) exhibited antinecrotic activity at 10 μ M (**Figure 5A**). Furthermore, compound **20** showed synergistic effects with necroptosis inhibitors including TAK632 (a RIPK1/3 inhibitor),[33] SZM630 (a RIPK3 inhibitor),[32] Nec-1 (a RIPK1 inhibitor),[6] and NSA (a MLKL inhibitor)[13] in TSZ-treated HT-29 cells, respectively (**Figure 5B**). The concentration used for CDDO was 10 μ M.

We next examined if compound **20** could inhibit Hsp90 in HT-29 cells by testing two biomarkers of Hsp90 inhibition. Consistent with other Hsp90 inhibitor, we found that compound **20** time-dependently induced reduction in the levels of a well-known Hsp90 client protein, EGFR and remarkable increases in the levels of Hsp70 (**Figure 5C**). They were both known to occur upon the inhibition of Hsp90.[46] Then, we examined phosphorylation of RIPK1, RIPK3, and MLKL in TSZ-treated HT-29 cells with or without **20**. As shown in **Figure 5C**, **20** could effectively inhibit the phosphorylation RIPK1, RIPK3, and MLKL. As the phosphorylation of RIPK1 and RIPK3 is required for RIPK1–RIPK3 necrosome formation,[12] we then explored the formation of necrosome in HT-29 cells after pretreating with **20**, and we found that it blocked TSZ-induced necrosome formation (**Figure 5D**). These data suggest that

compound **20** potentially targets Hsp90 not Nrf2 to block necrosome formation by inhibiting the phosphorylation of RIPK1 and RIPK3.

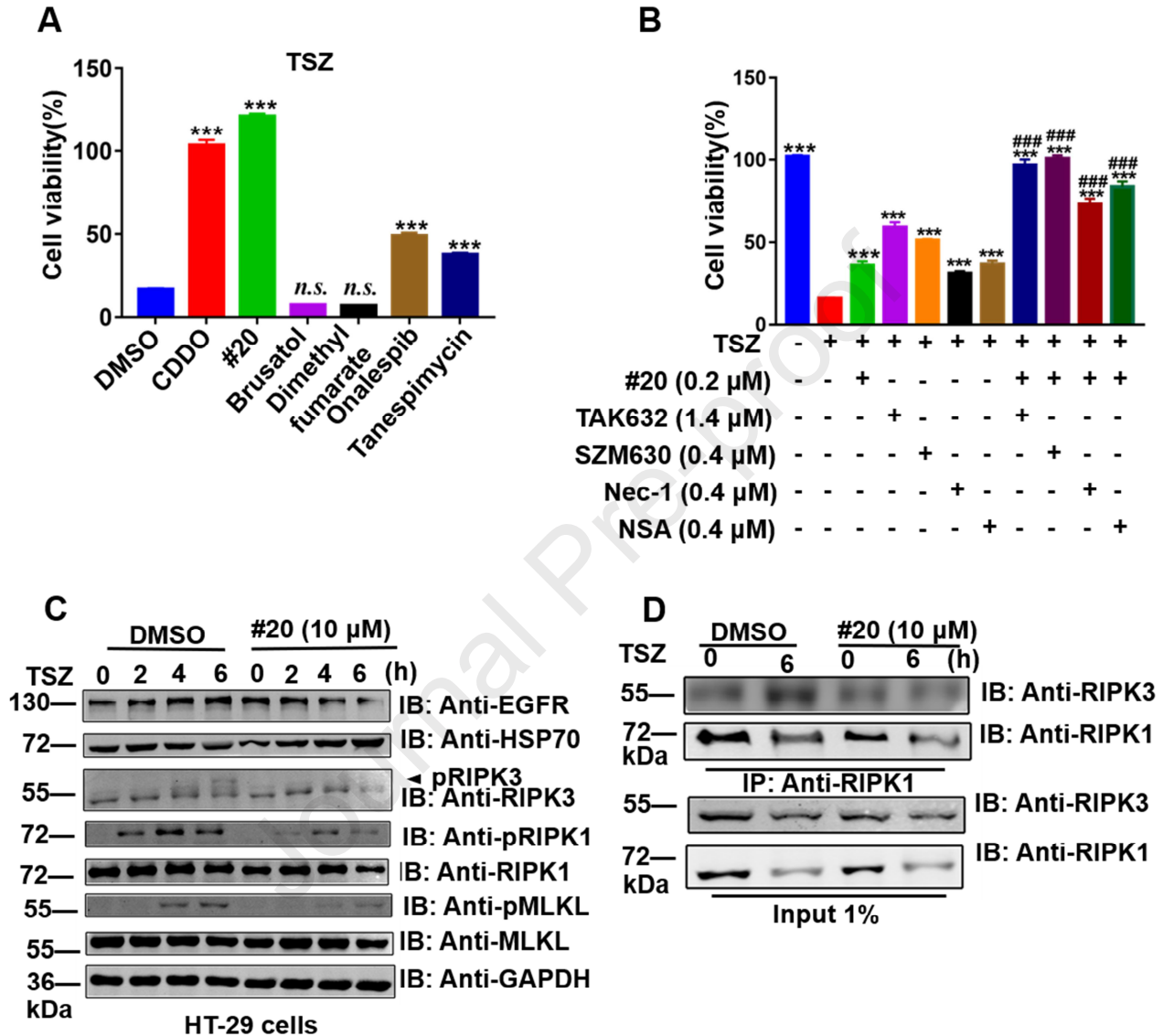


Figure 5. (A) HT-29 cells were treated with the indicated compounds at 10 μ M followed by stimulation with TSZ for 12 h. (B) HT-29 cells were treated with **20** combined by the indicated compounds followed by stimulation with TSZ for 12 h to evaluate the synergistic effects. (C) HT-29 cells were pre-treated with **20** (10 μ M) for 30 min and then treated with TSZ for the indicated periods of time. Cells were lysed and immunoblotted with the indicated antibodies. (D) HT-29 cells were treated with DMSO or **20** (10 μ M) for 6 h. The cell lysates were immunoprecipitated with an anti-RIPK1 antibody (IP:

RIPK1) and analyzed by immunoblotting with the indicated antibodies. (***) $p < 0.001$ versus TSZ simulation, ### $p < 0.001$ versus TSZ simulation with compound **20** treatment, n.s., not significant).

Compound 20 protects mice from TNF-induced systemic inflammatory response syndrome (SIRS). To explore whether compound **20** protects against RIP kinase-driven inflammation in vivo, we tested it in the TNF-induced SIRS model.[33] Compound **20** (10 or 20 mg/kg) given by intragastric gavage 2 h before i.v. injection of mTNF- α , protected mice from hypothermia (**Figure 6A**) and death (**Figure 6B**). Especially, the compound could completely reverse the mice from death at 20 mg/kg (100%). Furthermore, when these mice were examined at 6 h, the typical serum inflammatory cytokines including IL-1 β (**Figure 6C**) and IL-6 (**Figure 6D**) were markedly decreased after the treatment. Thus, these results demonstrate that compound **20** protects against TNF-induced SIRS in vivo.

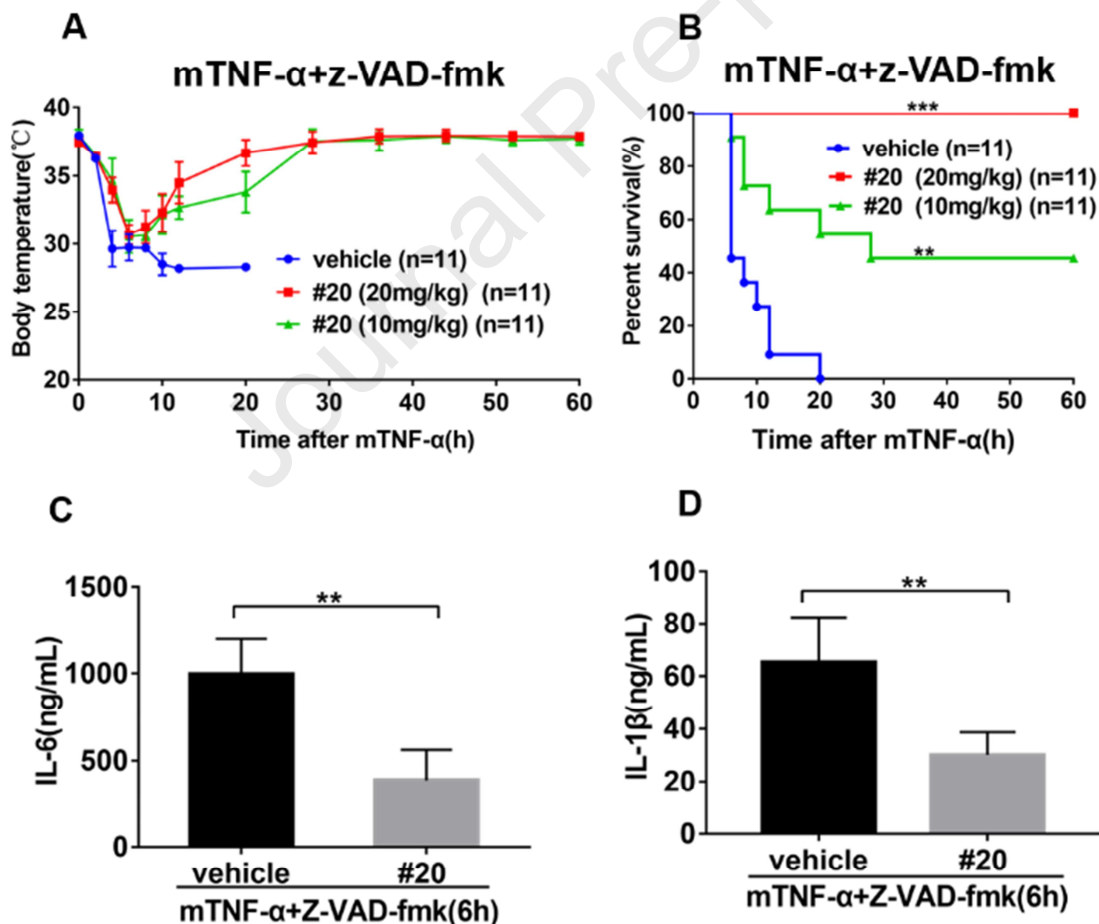


Figure 6. Compound 20 protects mice from TNF-induced SIRS. (A) C57BL/6 J mice were pre-treated with/out **20** (10, 20 mg/kg) and then the SIRS model was induced by TNF. The body tempera-

ture (means \pm S.E.M.) and (B) survival curve of the vehicle control and **20** treated mice (n=11 for each group) are shown. (C) After SIRS induction for 6 h, serum levels of IL-1 β , IL-6 from vehicle control and compound **20** (20 mg/kg) treated mice were determined by ELISA. *, $p < 0.05$; **, $p < 0.01$; ***, $p < 0.001$.

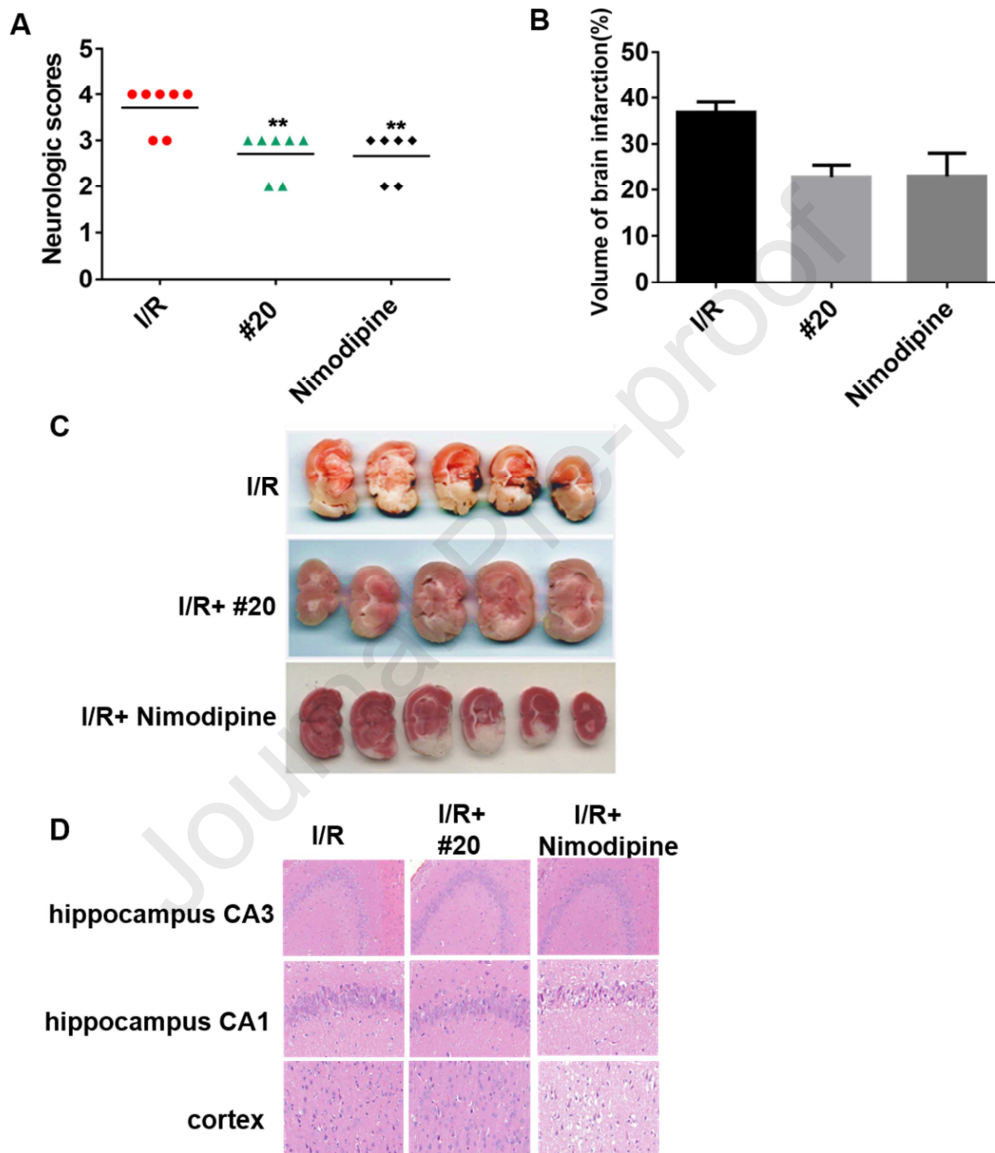


Figure 7. Compound **20** (100 mg/kg) protected against I/R injury in MCAO rats. (A) Neurological deficit scores, n = 6 per group. (B) The percentage of infarct volume was detected for each group, n = 6 per group. (C) Representative TTC staining of the cerebral infarct in brain, n = 6 per group. (D) HE staining: Ischemic cerebral cortex (magnification: $\times 200$), ischemic cerebral hippocampus CA3 (magnification: $\times 200$).

tion: $\times 100$) and ischemic cerebral hippocampus CA1 (magnification: $\times 200$), $n = 6$ per group. ($*p < 0.05$, $**p < 0.01$, $***p < 0.001$ versus the I/R group.)

Compound 20 protects brain against ischemia/reperfusion (I/R) injury. Extensive evidence suggests that necroptosis is a delayed component of ischemic neuronal injury, representing a promising therapeutic strategy for treatment of stroke.[6, 26, 47, 48] To examine the effect of potent compound **20** on the ischemic brain injury, we first examined the neurologic scores to determine neurological deficits after reperfusion for 24 h using middle cerebral artery occlusion (MCAO) rats. The neurological deficit score of **20**-treated group (100 mg/kg, score = 2.72 ± 0.45) was significantly decreased compared with the I/R group (score = 3.71 ± 0.45) (**Figure 7A**). The infarct volume of the cerebral ischemic area was measured by 2,3,5- triphenyltetrazolium chloride (TTC) staining. Pretreatment of **20** reduced infarct volume (**Figure 7B and C**). **20** reduced the infarct volume to $22.8 \pm 3.7\%$, comparable to that of nimodipine ($26.8 \pm 1.7\%$). Furthermore, the protective effect of **20** against was further determined by HE staining on sections from ischemic hippocampus and cortex at 24 h after reperfusion (**Figure 7D**). The number of cells in I/R group was decreased and arranged irregularly, and karyopyknosis was observed. In contrast, **20** pretreatment reversed the change of pathological to a certain extent, indicating that the compound protected brain from I/R injury.

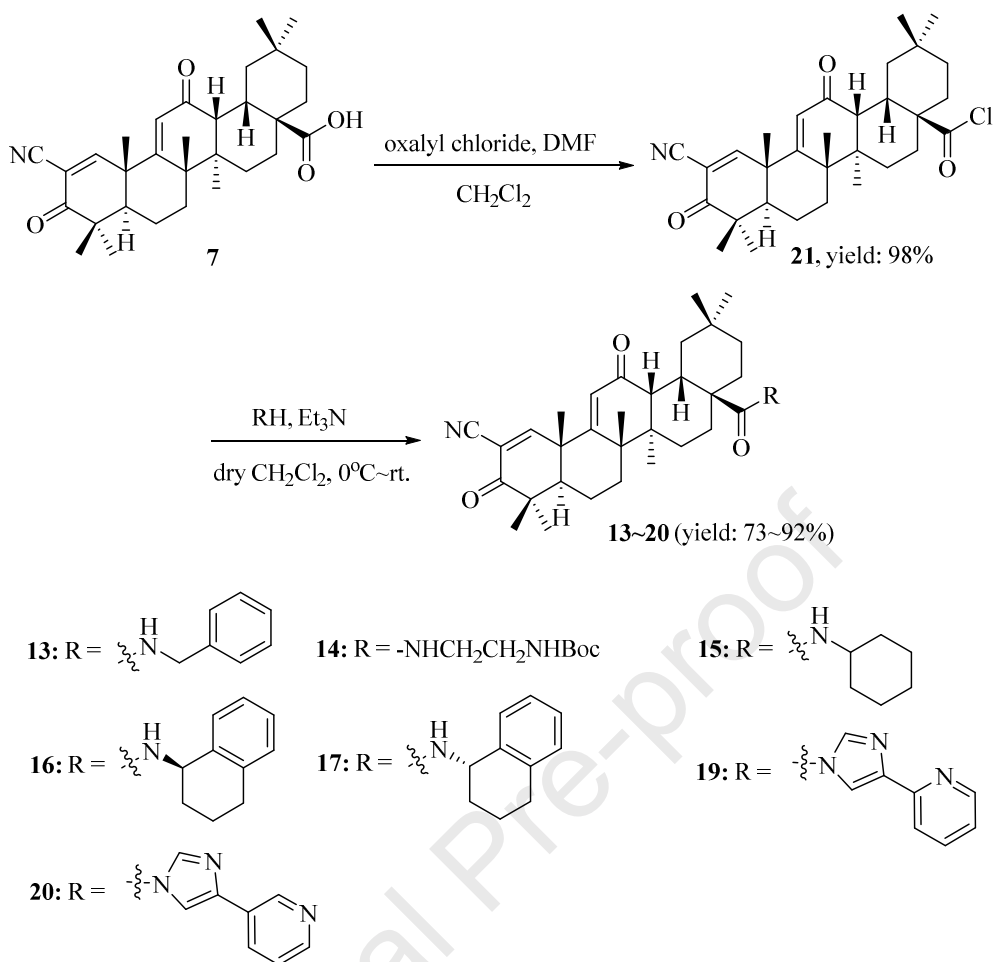
■ CONCLUSION

On the basis of CDDO scaffold, an inhibitor of necroptosis identified from an *in-house* natural product library, we developed a more potent analogue **20** by structural optimization. This compound could effectively protect against necroptosis in both human HT-29 and murine L929 cells. Compound **20** might target Hsp90 not Nrf2 to block necrosome formation by inhibiting the phosphorylation of RIPK1 and RIPK3. The antinecrototic effect of the compound could also be synergized with necroptosis inhibitors including TAK632 (a RIPK1/3 in-hibitor), SZM630 (a RIPK3 inhibitor), Nec-1 (a RIPK1 in-hibitor), and NSA (a MLKL inhibitor). Intragastric administration of this compound alleviates TNF-induced

SIRS by significantly decreasing the serum levels of IL-1 β and IL-6. It was also orally effective toward cerebral I/R injury in rat models. Our results suggest that compound **20** could be a lead compound for discovering more necroptosis inhibitors in I/R treatment, providing a unique opportunity to characterize the role of necroptosis in I/R or other human pathologies.

■ EXPERIMENTAL SECTION

Chemistry. General Methods. All solvents and starting materials, including anhydrous solvents and chemicals, were purchased from commercial vendors and used without any further purification. TLC analysis was carried out on silica gel plates GF254 (Qindao Haiyang Chemical, China). Column chromatography was carried out on silica gel 300~400 mesh. Nuclear magnetic resonance (^1H NMR, ^{13}C NMR) spectra were recorded in CDCl_3 on a Bruker Avance 600 spectrometer (Bruker Company, Germany). Chemical shifts (δ values) and coupling constants (J values) are given in ppm and Hz, respectively, using tetramethylsilane (TMS) as an internal standard; splitting patterns are designated as follows: s, singlet; d, doublet; t, triplet; q, quadruplet; m, multiplet; dd, double doublet; dt, double triplet. MS spectra were recorded on a Mariner Mass Spectrum (ESI) on Agilent Technologies LC/MSD TOF. The final structures were fully characterized by ^1H NMR, ^{13}C NMR, and MS (ESI). Purities of all the test compounds were >95% determined by high-performance liquid chromatography (HPLC, Agilent Technologies 1200 Series) analysis using methanol or acetonitrile /water as the mobile phase with a flow rate of 0.5 or 2.0 mL/min on a C18 column (YMC-Pack ODS-A, 5 μm , 250 \times 10 mmI.D.).



Scheme 1. Synthetic route for CDDO derivatives.

In tested compounds, **7** (CAS: 218600-44-3), **8** (CAS: 508-02-1) and **9** (CAS: 510-30-5) were purchased from Tokyo Chemical Industry (TCI) and Aladdin Company. Brusatol (CAS: 14907-98-3) and dimethyl fumarate (CAS: 624-49-7), Onalespib (CAS: 912999-49-6) and Luminespib (CAS: 747412-49-3) were purchased from Targetmol (Targetmol, USA). Compound **10** (CAS: 218600-53-4), **11** (CAS: 932730-51-3), **12** (CAS: 1474034-05-3) and **18** (CAS: 443104-02-7) were purchased from MedChemExpress company (<https://www.medchemexpress.cn/>). The HPLC purity of the compounds were >98%. Compounds **13-17**, **19-20** were synthesized and the synthetic routes of the target compounds were depicted in **Scheme 1**. The first key intermediates (acyl chloride, **21**) were prepared using commercially available bardozone **7**. Then, the intermediate **21** was reacted with amines using a simple substitution reaction to provide target compounds.

2-cyano-3,12-dioxooleana-1,9(11)-dien-28-N-benzylformamide (13).[49] To a solution of bardoxolone (CDDO, 30 mg, 0.06 mmol) in dry dichloromethane, oxalyl chloride (16 μ L, 0.18 mmol) and catalytic amount of DMF was added. The mixture was stirred at 23 ± 2 °C for 2~5 h before the solvent was removed. The residue was dried under vacuum, then used to the next step without any purification. The residue was mixed with trimethylamine (16 μ L, 0.11 mmol) in DCM and then cooled to 0 °C for 10 min. Then the benzylamine (20 μ L, 0.18 mmol) was added dropwise. The mixture was stirred at 0 °C for 4 h and then extracted with DCM. The organic layer was separated, washed with brine and dried over sodium sulfate. The combined organic layers were evaporated to dryness to obtain the crude product, which was purified by column chromatography on silica gel using PE/EtOAc (5:1) as eluent to obtain product as white solid (25.0 mg, yield: 73.5%), mp 186-188 °C. CAS: 443103-59-1. ^1H NMR (600 MHz, CDCl_3) δ : 0.90 (s, 3H, CH_3), 0.99 (s, 6H, $2 \times \text{CH}_3$), 1.15 (s, 3H, CH_3), 1.16 (s, 3H, CH_3), 1.24 (s, 3H, CH_3), 1.46 (s, 3H, CH_3), 1.83-1.88 (m, 1H, CH), 1.96-2.01 (m, 1H, CH), 2.91-2.93 (m, 1H, H-18), 3.01 (d, 1H, $J = 4.4$ Hz, H-13), 4.43-4.51 (m, 2H, NCH_2), 5.96 (s, 1H, H-11), 6.18-6.20 (m, 1H, NH), 7.26-7.30 (m, 5H, $5 \times \text{ArH}$), 8.04 (s, 1H, H-1). ^{13}C NMR (150 MHz, CDCl_3) δ : 18.2, 21.6, 21.7, 23.1, 24.7, 26.6, 27.0, 27.7, 30.4, 30.6, 31.7, 32.0, 33.3, 34.1, 34.6, 36.1, 42.1, 42.5, 43.7, 45.0, 45.8, 46.5, 47.7, 49.5, 114.4, 114.6, 124.0 (CN), 127.4 ($\text{C}_p\text{-Ph}$), 128.0 ($\text{C}_o\text{-Ph}$), 128.7 ($\text{C}_m\text{-Ph}$), 138.8 ($\text{C}_i\text{-Ph}$), 165.8, 168.7, 176.9 (C-28), 196.6 (C-3), 199.0 (C-12). MS (ESI): 581.402 [$\text{M}+\text{H}$] $^+$, 603.343 [$\text{M}+\text{Na}$] $^+$, 619.317 [$\text{M}+\text{K}$] $^+$. HPLC purity: 97.7%, $R_t = 8.690$ min, UV 254 nm, 95% methanol, flowrate: 2.0 mL/min.

***Tert*-butyl(2-(2-cyano-3,12-dioxooleana-1,9(11)-dien-28-amide)ethyl)carbamate (14).** White solid (58.2 mg, yield: 92%), mp 195-197 °C. ^1H NMR (600 MHz, CDCl_3) δ : 0.92 (s, 3H, CH_3), 1.02 (s, 3H, CH_3), 1.04 (s, 3H, CH_3), 1.10 (s, 3H, CH_3), 1.28 (s, 3H, CH_3), 1.36 (s, 3H, CH_3), 1.47 (s, 9H, $3 \times \text{CH}_3$), 1.50 (s, 3H, CH_3), 1.83-1.86 (m, 1H, CH), 2.01-2.06 (m, 1H, CH), 2.97-2.99 (m, 1H, H-18), 3.10-3.11 (m, 1H, H-13), 3.28-3.34 (m, 2H, CH_2N), 3.35-3.42 (m, 2H, NCH_2), 6.00 (s, 1H, H-11), 6.85 (s, 1H, NH), 8.08 (s, 1H, H-1). ^{13}C NMR (150 MHz, CDCl_3) δ : 14.2, 18.2, 21.6, 21.7, 23.0, 23.1, 24.8, 26.6, 27.0, 27.8, 28.4, 30.6, 31.7, 33.3, 34.0, 34.6, 36.0, 42.1, 42.5, 45.0, 45.9, 46.4, 47.7, 49.4, 60.4, 114.4,

114.6, 124.0 (CN), 157.2, 165.8, 171.2 (NCOO), 178.1 (C-28), 196.6 (C-3), 199.0 (C-12). MS (ESI): 656.428 [M+Na]⁺, 672.394 [M+K]⁺. HPLC purity: 97.5%, R_t = 8.726 min, UV 254 nm, 95% methanol, flowrate: 2.0 mL/min.

2-cyano-3,12-dioxoleana-1,9(11)-dien-28-N-cyclohexylformamide (15). White solid (43 mg, yield: 74%), mp 187-189 °C. CAS: 1788897-54-0. ¹H NMR (600 MHz, CDCl₃) δ: 0.90 (s, 3H, CH₃), 0.99 (s, 3H, CH₃), 1.01(s, 3H, CH₃), 1.18 (s, 3H, CH₃), 1.25 (s, 3H, CH₃), 1.31 (s, 3H, CH₃), 1.34-1.39 (m, 4H, 2×CH₂), 1.48 (s, 3H, CH₃), 1.94-1.99 (m, 1H, CH), 2.85-2.87 (m, 1H, H-18), 3.06 (d, 1H, J = 4.6 Hz, H-13), 3.80-3.82 (m, 1H, NCH), 5.58 (d, 1H, J = 7.8 Hz, NH), 5.97 (s, 1H, H-11), 8.04 (s, 1H, H-1). ¹³C NMR (150 MHz, CDCl₃) δ: 18.2, 21.6, 21.7, 23.0, 23.1, 24.9, 25.0, 25.5, 26.6, 27.0, 27.8, 30.6, 31.7, 32.0, 33.2, 33.3, 33.3, 34.2, 34.6, 36.1, 42.1, 42.5, 45.0, 46.0, 46.3, 47.7, 48.0, 49.5, 114.4, 114.6, 124.0 (CN), 165.7, 168.6, 176.0 (C-28), 196.6 (C-3), 199.0 (C-12). MS (ESI): 573.467 [M+H]⁺, 595.398 [M+Na]⁺. HPLC purity: > 99%, R_t = 9.718 min, UV 254 nm, 95% methanol, flowrate: 2.0 mL/min.

(R)-1-N-(2-cyano-3,12-dioxoleana-1,9(11)-dien-28-amide)-1,2,3,4-tetrahydronaphthalene (16). White solid (52 mg, yield: 83.8%), mp 205-207 °C. CAS: 2490323-21-0. ¹H NMR (600 MHz, CDCl₃) δ: 0.90 (s, 3H, CH₃), 0.96 (s, 3H, CH₃), 1.02 (s, 3H, CH₃), 1.18 (s, 3H, CH₃), 1.26 (s, 3H, CH₃), 1.29-1.36 (m, 2H, CH₂), 1.40 (s, 3H, CH₃), 1.50 (s, 3H, CH₃), 1.94-2.04 (m, 2H, CH₂), 2.73-2.85 (m, 3H, CH₂, H-18), 3.07 (d, 1H, J = 4.7 Hz, H-13), 5.20-5.23 (m, 1H, NCH), 5.95 (d, 1H, J = 8.2 Hz, NH), 5.97 (s, 1H, H-11), 7.12-7.26 (m, 4H, 4×ArH), 8.03 (s, 1H, H-1). ¹³C NMR (150 MHz, CDCl₃) δ: 18.3, 20.1, 21.6, 21.8, 22.9, 23.1, 25.0, 26.7, 27.0, 27.8, 29.3, 30.4, 30.6, 31.7, 32.1, 33.2, 34.2, 34.6, 36.2, 42.2, 42.6, 45.0, 46.0, 46.6, 47.3, 47.7, 49.6, 114.7, 114.4, 124.0 (CN), 126.4, 127.4, 128.4, 129.4, 136.8, 137.8, 165.6, 168.8, 176.2 (C-28), 196.5 (C-3), 198.8 (C-12). MS (ESI): 621.416 [M+H]⁺, 643.386 [M+Na]⁺, 659.359 [M+K]⁺. HPLC purity: 95.0%, R_t = 8.796 min, UV 254 nm, 90% methanol, flowrate: 2.0 mL/min.

(S)-1-N-(2-cyano-3,12-dioxoleana-1,9(11)-dien-28-amide)-1,2,3,4-tetrahydronaphthalene (17). White solid (45 mg, yield: 73%), mp 185-186 °C. CAS: 2490323-22-1. ¹H NMR (600 MHz, CDCl₃) δ:

0.90 (s, 3H, CH₃), 1.01 (s, 3H, CH₃), 1.02(s, 3H, CH₃), 1.17 (s, 3H, CH₃), 1.26 (s, 3H, CH₃), 1.17-1.33 (m, 2H, CH₂), 1.39 (s, 3H, CH₃), 1.49 (s, 3H, CH₃), 2.05-2.08 (m, 2H, CH₂), 2.75-2.86 (m, 2H, CH₂), 3.01-3.03 (m, 1H, H-18), 3.16 (d, 1H, $J = 4.7$ Hz, H-13), 5.20-5.23 (m, 1H, NCH), 5.91 (d, 1H, $J = 8.0$ Hz, NH), 5.96 (s, 1H, H-11), 7.10-7.27 (m, 4H, 4×ArH), 8.04 (s, 1H, H-1). ¹³C NMR (150 MHz, CDCl₃) δ : 18.2, 20.2, 21.6, 21.6, 23.1, 23.4, 24.9, 26.7, 27.0, 27.8, 29.3, 30.4, 30.6, 31.7, 32.2, 33.3, 34.2, 34.7, 36.0, 42.2, 42.5, 45.0, 46.0, 46.4, 47.4, 47.7, 49.4, 114.4, 114.6 124.1 (CN), 126.3, 127.3, 128.4, 129.3, 136.7, 137.7, 165.8, 168.1, 176.1 (C-28), 196.6 (C-3), 198.8 (C-12). MS (ESI): 621.393 [M+H]⁺. HPLC purity: 98.7%, $R_t = 10.135$ min, UV 254 nm, 95% methanol, flowrate: 2.0 mL/min.

1-(2-cyano-3,12-dioxooleana-1,9(11)-dien-28-oyl)-4-(pyridin-2-yl)-1H-imidazole (19). White solid (25 mg, yield: 89%), mp 197-199 °C. CAS: 1883650-96-1. ¹H NMR (400 MHz, DMSO-*d*₆) δ : 0.93 (s, 3H, CH₃), 0.95 (s, 3H, CH₃), 0.99(s, 3H, CH₃), 1.04 (s, 3H, CH₃), 1.15 (s, 3H, CH₃), 1.21 (s, 3H, CH₃), 1.42 (s, 3H, CH₃), 2.99-3.03 (m, 1H, H-18), 3.12 (d, 1H, $J = 4.4$ Hz, H-13), 6.26 (s, 1H, H-11), 7.31-7.34 (m, 1H, Ar-H), 7.88-7.97 (m, 2H, Ar-H), 8.26 (s, 1H, H-1), 8.58 (m, 1H, Ar-H), 8.68 (s, 1H, Ar-H), 8.74 (s, 1H, Ar-H). ¹³C NMR (150 MHz, CDCl₃) δ : 18.2, 21.4, 21.5, 23.2, 23.5, 24.4, 26.6, 26.9, 28.5, 30.3, 31.6, 32.6, 32.8, 34.3, 35.6, 42.4, 42.5, 45.0, 45.8, 47.8, 48.6, 50.0, 113.4, 114.3, 114.6, 122.9, 124.1 (CN), 128.9, 133.4, 138.2, 139.5, 146.2, 148.1, 165.5, 168.0, 175.2 (C-28), 196.4 (C-3), 198.3 (C-12). MS (ESI): 619.365 [M+H]⁺. HPLC purity: 98.1%, $R_t = 6.538$ min, UV 210 nm, 90% acetonitrile, flowrate: 1.0 mL/min

1-(2-cyano-3,12-dioxooleana-1,9(11)-dien-28-oyl)-4-(pyridin-3-yl)-1H-imidazole (20). White solid (37 mg, yield: 92%), mp 193-195 °C. CAS NO. 1883650-95-0. ¹H NMR (400 MHz, DMSO-*d*₆) δ : 0.95 (s, 6H, 2×CH₃), 1.00 (s, 3H, CH₃), 1.08 (s, 3H, CH₃), 1.16 (s, 3H, CH₃), 1.20 (s, 3H, CH₃), 1.43 (s, 3H, CH₃), 3.16-3.18 (m, 1H, H-18), 3.35 (d, 1H, $J = 4.0$ Hz, H-13), 6.26 (s, 1H, H-11), 7.44 (dd, 1H, $J = 4.0$ Hz, 7.9 Hz, Ar-H), 8.28 (d, 1H, $J = 8.0$ Hz, Ar-H), 8.50 (d, 1H, $J = 4.8$ Hz, Ar-H), 8.59 (s, 1H, H-1), 8.68 (s, 1H, Ar-H), 8.72 (s, 1H, Ar-H), 9.16 (s, 1H, Ar-H). ¹³C NMR (150 MHz, CDCl₃) δ : 18.2, 21.6, 23.6, 23.7, 24.5, 26.6, 26.9, 28.4, 30.4, 31.6, 31.9, 32.7, 32.8, 34.3, 35.6, 42.3, 42.5, 45.0, 45.8, 47.8,

48.7, 50.0, 113.4, 114.3, 114.7, 123.9, 124.0 (CN), 128.9, 133.4, 137.8, 139.4, 146.1, 148.1, 165.4, 168.1, 174.8 (C-28), 196.4 (C-3), 198.1 (C-12). MS (ESI): 619.366 [M+H]⁺. HPLC purity: > 99%, R_t = 12.983 min, UV 210 nm, 30~90% acetonitrile, flowrate: 0.5 mL/min

Biology

Reagents

Dulbecco's modified Eagle's medium (DMEM), fetal bovine serum (FBS), penicillin–streptomycin liquid (100×), phosphate buffer saline (PBS). The 2,3,5-triphenyl tetrazolium chloride (TTC) was obtained from BIO BASICINC (Shanghai, China). Recombinant mouse/human TNF- α were purchased from Novoprotein (Shanghai, China).

Cell culture and Transfection

HT-29 (NCI-DTP Cat# HT-29), L929 (ECACC Cat# 14112101) cells were cultured in DMEM with 10% FBS (v/v), 1% L-glutamine and 100 U/mL penicillin/streptomycin(v/v). Cells were grown at 37 °C in a humidified atmosphere with 5 % CO₂ and were harvested in all experiments from exponentially growing cultures.

Necroptosis induction and cell viability assays

Necroptosis was induced by pre-treatment with z-VAD-fmk (20 μ M) and Smac mimetic (10 μ M) or cycloheximide (5 μ g/mL) for 30 min and followed by TNF- α (20 ng/mL) for 12 or 16 h. Apoptosis was induced by TNF- α (20 ng/mL) and Smac mimetic (10 nM) for 24 h. The compounds were incubated with the cells exposed to one of the above combinations at the indicated concentrations for 16 h or 24 h. Cell viability was then examined by using the CellTiter-Glo Luminescent Cell Viability Assay kit.

SIRS mouse model

All animal experiments were performed in accordance with the National Institutes of Health guidelines and approved by the animal care and use committee of the Second Military Medical University (EC11-055). For TNF-induced SIRS, female C57BL/6 J mice (6–8 weeks old) were purchased from Changzhou Caven Laboratory Animal (Jiangsu, China) and raised in a pathogen-free environment (21–26 °C and 40–70 % humidity). Compounds were suspended in 0.5% carboxymethyl cellulose sodium. Over-

night-fasted mice were randomized divided into vehicle and treatment groups (n=11 for each group). In drug treatment groups, mice were given the test compound with different concentrations by oral gavage 2 h before TNF injection. mTNF- α was diluted in endotoxin-free PBS and intravenously injected (250 $\mu\text{g}/\text{kg}$) in a volume of 200 μL . Z-VAD-fmk was intraperitoneally given 200 μg 15 min before, and 75 μg 1 h after mTNF- α treatment. Body temperature was monitored with an electric thermometer.

MCAO rat model and treatment with CDDO analogues

Healthy adult male Sprague-Dawley rats weighing 180–220 g were purchased from Changzhou Caven Laboratory Animal (Jiangsu, China) and raised in a pathogen-free environment (21–26 °C and 40–70 % humidity). Rats were anesthetized with 10% chloral hydrate (300 mg / kg, i.p.), monofilament nylon suture was inserted into the internal carotid artery (ICA), and then it was advanced to block the left middle cerebral artery (MCA). After 2 h of occlusion, the thread was dismantled carefully to achieve the reperfusion for 24 h. Sham-operated mice were exposed to the same surgical procedure, except for arteries occlusion. All rats were divided randomly into four groups as follows using a random number table: sham operated (sham), I/R (vehicle), I/R + compound **20** (100 mg/kg), and I/R + nimodipine (1 mg/kg) groups. Nimodipine, as the first-line treatment for stroke, an L-type voltage-gated calcium channel, caused vasodilatation of vascular smooth muscle cells.[50, 51] Thus, nimodipine was used as a positive control.

Neurological Deficit Score

Neurological deficits were evaluated blindly after 24 h of reperfusion with Zea-Longa score scoring system.[52] The scoring system is as follows: 0 = No signs of impaired nerve function, normal activity; 1 = Cannot fully extend contralateral forepaws; 2 = Circle to the opposite side while walking; 3 = Dump to the opposite side; 4 = Cannot go away spontaneously and lose consciousness.

Infarct Volume Evaluation

After 24 h of reperfusion, six animals of each group were euthanized by cervical dislocation and decapitated, then brains were used to measure infarct volume immediately. The animal brains were cut into 2 mm thick coronal sections, 5 - 6 pieces and exposed to TTC staining after immersion in 4% paraformal-

dehyde for 4 h at 4 °C. Unstained areas were defined as infarcts and measured using microscope image-analysis software (Image-Pro Plus, U.S.A.). The proportion of cerebral infarction was calculated as follows: Proportion of cerebral infarction (%) = Infarct area / whole brain area ×100%).

Hematoxylin-Eosin (HE) Staining

Rats were anesthetized with 10% chloral hydrate after 24 h of reperfusion, perfused with physiological saline and 4% paraformaldehyde and then decapitated. Brains were dehydrated and embedded in paraffin and then cut into 5 µm coronal sections; subsequently, brain sections were deparaffinized and hydrated for HE staining.

Western Blotting

After CDDO analogues treatment, the protein samples were extracted from cells using RIPA lysis buffer containing a protease inhibitor and phosphatase inhibitor cocktail (Beyotime Biotechnology, China). The quantification of proteins was analyzed using BCA protein assay kit (Beyotime Biotechnology, China). The proteins (30 µg) were resolved over sodium dodecyl sulfate-polyacrylamide gel electrophoresis (SDS-PAGE) and transferred to PVDF membranes (Millipore, Bedford, MA, U.S.A.). Then, the membranes were blocked in 5% BSA for 2 h. Primary antibodies were prepared in 1% BSA at a dilution of 1:1000. The blocked membranes were incubated with corresponding antibody overnight at 4°C, followed by the incubation with marked secondary antibody (1:8000) for 1 h at room temperature. The signals were captured and analyzed using the LI-COR Odyssey system. Antibodies were from commercial sources: anti-RIPK1 (Abcam Cat# ab178420); anti-human phospho-RIPK1 (Cell Signaling Technology, Cat# 65746); anti-human-RIPK3 (Abcam Cat# ab56164), anti-human phospho-RIPK3 (Abcam Cat# ab209384), anti-human MLKL (Abcam Cat# ab184718), anti-human phospho-MLKL (Abcam Cat# ab187091), anti-GAPDH (Abcam Cat# ab181602). Anti-HSP70 (CST Cat# 4872), anti-EGFR (CST Cat# 4267).

Immunoprecipitation

Cells were lysed with Nonidet P-40 buffer (Beyotime Biotechnology, China) supplemented with 1 mM PMSF, 1× protease inhibitor mixture (Roche), 10 mM β-glycerophosphate, 5 mM NaF, and 1 mM

Na₃VO₄. The lysates were centrifuged and the supernatants were incubated with anti-RIPK1 (CST Cat# 3493S) antibody overnight at 4 °C. The immunocomplex was captured by Protein A/G Agarose (Life Technologies) overnight at 4 °C. Beads were washed three times with PBS, and the bound proteins were removed by boiling in SDS buffer, and the samples were resolved in 10% SDS-polyacrylamide gels by western blotting analysis.

Statistical Analysis.

The one-way analysis of variance was used to compare differences among groups represented by the mean values ± SD. A log-rank (Mantel–Cox) test was performed for survival curve analysis. P < 0.05 was considered statistically significant.

ASSOCIATED CONTENT

Supporting Information

¹H, ¹³C NMR spectra, MS, and HPLC of target compounds (DOCX).

ACKNOWLEDGMENTS

This work was funded by grants from the National Natural Science Foundation of China (82022065, 81872791, 82073696, 81872880 and 81973551); the Key Research and Development Program of Ningxia (2019BFG02017).

ABBREVIATIONS USED

ACD, accidental cell death; CDDO, bardoxolone; I/R, ischemia/reperfusion; HPLC, high-performance liquid chromatography; MCAO, middle cerebral artery occlusion; MLKL, mixed lineage kinase domain-like protein; PCD, programmed cell death; PDAC, pancreatic ductal adenocarcinoma cancer; RIPK1, receptor-interacting protein kinase 1; RIPK3, receptor-interacting protein kinase 3; SIRS, systemic inflammatory response syndrome; TC, TNF-α and cycloheximide; TCZ, TNF-α, cycloheximide, and z-VAD-fmk; TNF-α, tumor necrosis factor-α; TS, TNF-α and Smac mimetic; TSZ, TNF-α, Smac mimetic, and z-VAD-fmk; TTC, 2,3,5-triphenyltetrazolium chloride; TZ, TNF-α and z-VAD-fmk; UC, ulcerative colitis

REFERENCES

- [1] N.N. Danial, S.J. Korsmeyer, Cell death: critical control points, *Cell* 2004;116: 205-219.
- [2] J.F. Kerr, A.H. Wyllie, A.R. Currie, Apoptosis: a basic biological phenomenon with wide-ranging implications in tissue kinetics, *Br J Cancer* 1972;26: 239-257.
- [3] J. Yuan, H.R. Horvitz, A first insight into the molecular mechanisms of apoptosis, *Cell* 2004;116: S53-56, 51 p following S59.
- [4] T. Vanden Berghe, A. Linkermann, S. Jouan-Lanhouet, H. Walczak, P. Vandenabeele, Regulated necrosis: the expanding network of non-apoptotic cell death pathways, *Nat Rev Mol Cell Biol* 2014;15: 135-147.
- [5] P. Vandenabeele, L. Galluzzi, T. Vanden Berghe, G. Kroemer, Molecular mechanisms of necroptosis: an ordered cellular explosion, *Nat Rev Mol Cell Biol* 2010;11: 700-714.
- [6] A. Degterev, Z. Huang, M. Boyce, Y. Li, P. Jagtap, N. Mizushima, G.D. Cuny, T.J. Mitchison, M.A. Moskowitz, J. Yuan, Chemical inhibitor of nonapoptotic cell death with therapeutic potential for ischemic brain injury, *Nat Chem Biol* 2005;1: 112-119.
- [7] M. Pasparakis, P. Vandenabeele, Necroptosis and its role in inflammation, *Nature* 2015;517: 311-320.
- [8] A. Degterev, J. Hitomi, M. Germscheid, I.L. Ch'en, O. Korkina, X. Teng, D. Abbott, G.D. Cuny, C. Yuan, G. Wagner, S.M. Hedrick, S.A. Gerber, A. Lugovskoy, J. Yuan, Identification of RIP1 kinase as a specific cellular target of necrostatins, *Nat Chem Biol* 2008;4: 313-321.
- [9] M. Jaattela, J. Tschopp, Caspase-independent cell death in T lymphocytes, *Nat Immunol* 2003;4: 416-423.
- [10] S. Grootjans, T. Vanden Berghe, P. Vandenabeele, Initiation and execution mechanisms of necroptosis: an overview, *Cell Death Differ* 2017;24: 1184-1195.
- [11] S. He, L. Wang, L. Miao, T. Wang, F. Du, L. Zhao, X. Wang, Receptor interacting protein kinase-3 determines cellular necrotic response to TNF-alpha, *Cell* 2009;137: 1100-1111.

- [12] Y.S. Cho, S. Challa, D. Moquin, R. Genga, T.D. Ray, M. Guildford, F.K. Chan, Phosphorylation-driven assembly of the RIP1-RIP3 complex regulates programmed necrosis and virus-induced inflammation, *Cell* 2009;137: 1112-1123.
- [13] L. Sun, H. Wang, Z. Wang, S. He, S. Chen, D. Liao, L. Wang, J. Yan, W. Liu, X. Lei, X. Wang, Mixed lineage kinase domain-like protein mediates necrosis signaling downstream of RIP3 kinase, *Cell* 2012;148: 213-227.
- [14] J. Zhao, S. Jitkaew, Z. Cai, S. Choksi, Q. Li, J. Luo, Z.G. Liu, Mixed lineage kinase domain-like is a key receptor interacting protein 3 downstream component of TNF-induced necrosis, *Proc Natl Acad Sci U S A* 2012;109: 5322-5327.
- [15] Z. Cai, S. Jitkaew, J. Zhao, H.C. Chiang, S. Choksi, J. Liu, Y. Ward, L.G. Wu, Z.G. Liu, Plasma membrane translocation of trimerized MLKL protein is required for TNF-induced necroptosis, *Nat Cell Biol* 2014;16: 55-65.
- [16] X. Chen, W. Li, J. Ren, D. Huang, W.T. He, Y. Song, C. Yang, W. Li, X. Zheng, P. Chen, J. Han, Translocation of mixed lineage kinase domain-like protein to plasma membrane leads to necrotic cell death, *Cell Res* 2014;24: 105-121.
- [17] Y. Dondelinger, W. Declercq, S. Montessuit, R. Roelandt, A. Goncalves, I. Bruggeman, P. Hulpiau, K. Weber, C.A. Sehon, R.W. Marquis, J. Bertin, P.J. Gough, S. Savvides, J.C. Martinou, M.J. Bertrand, P. Vandenabeele, MLKL compromises plasma membrane integrity by binding to phosphatidylinositol phosphates, *Cell Rep* 2014;7: 971-981.
- [18] H. Wang, L. Sun, L. Su, J. Rizo, L. Liu, L.F. Wang, F.S. Wang, X. Wang, Mixed lineage kinase domain-like protein MLKL causes necrotic membrane disruption upon phosphorylation by RIP3, *Mol Cell* 2014;54: 133-146.
- [19] D. Wallach, T.B. Kang, C.P. Dillon, D.R. Green, Programmed necrosis in inflammation: Toward identification of the effector molecules, *Science* 2016;352: aaf2154.
- [20] C. Zhuang, F. Chen, Small-Molecule Inhibitors of Necroptosis: Current Status and Perspectives, *J Med Chem* 2020;63: 1490-1510.

- [21] M. Yoshikawa, M. Saitoh, T. Katoh, T. Seki, S.V. Bigi, Y. Shimizu, T. Ishii, T. Okai, M. Kuno, H. Hattori, E. Watanabe, K.S. Saikatendu, H. Zou, M. Nakakariya, T. Tatamiya, Y. Nakada, T. Yogo, Discovery of 7-oxo-2,4,5,7-tetrahydro-6 h-pyrazolo[3,4- c]pyridine derivatives as potent, orally available, and brain-penetrating receptor interacting protein 1 (RIP1) kinase inhibitors: analysis of structure-kinetic relationships, *J Med Chem* 2018;61: 2384-2409.
- [22] P.A. Harris, B.W. King, D. Bandyopadhyay, S.B. Berger, N. Campobasso, C.A. Capriotti, J.A. Cox, L. Dare, X. Dong, J.N. Finger, L.C. Grady, S.J. Hoffman, J.U. Jeong, J. Kang, V. Kasparcova, A.S. Lakdawala, R. Lehr, D.E. McNulty, R. Nagilla, M.T. Ouellette, C.S. Pao, A.R. Rendina, M.C. Schaeffer, J.D. Summerfield, B.A. Swift, R.D. Totoritis, P. Ward, A. Zhang, D. Zhang, R.W. Marquis, J. Bertin, P.J. Gough, DNA-encoded library screening identifies benzo[b][1,4]oxazepin-4-ones as highly potent and monoselective receptor interacting protein 1 kinase inhibitors, *J Med Chem* 2016;59: 2163-2178.
- [23] P.A. Harris, S.B. Berger, J.U. Jeong, R. Nagilla, D. Bandyopadhyay, N. Campobasso, C.A. Capriotti, J.A. Cox, L. Dare, X. Dong, P.M. Eidam, J.N. Finger, S.J. Hoffman, J. Kang, V. Kasparcova, B.W. King, R. Lehr, Y. Lan, L.K. Leister, J.D. Lich, T.T. MacDonald, N.A. Miller, M.T. Ouellette, C.S. Pao, A. Rahman, M.A. Reilly, A.R. Rendina, E.J. Rivera, M.C. Schaeffer, C.A. Schon, R.R. Singhaus, H.H. Sun, B.A. Swift, R.D. Totoritis, A. Vossenkamper, P. Ward, D.D. Wisnoski, D. Zhang, R.W. Marquis, P.J. Gough, J. Bertin, Discovery of a first-in-class receptor interacting protein 1 (RIP1) kinase specific clinical candidate (GSK2982772) for the treatment of inflammatory diseases, *J Med Chem* 2017;60: 1247-1261.
- [24] K. Weisel, N.E. Scott, D.J. Tompson, B.J. Votta, S. Madhavan, K. Povey, A. Wolstenholme, M. Simeoni, T. Rudo, L. Richards-Peterson, T. Sahota, J.G. Wang, J. Lich, J. Finger, A. Verticelli, M. Reilly, P.J. Gough, P.A. Harris, J. Bertin, M.L. Wang, Randomized clinical study of safety, pharmacokinetics, and pharmacodynamics of RIPK1 inhibitor GSK2982772 in healthy volunteers, *Pharmacol Res Perspect* 2017;5: e00365.
- [25] P.A. Harris, J.M. Marinis, J.D. Lich, S.B. Berger, A. Chirala, J.A. Cox, P.M. Eidam, J.N. Finger, P.J. Gough, J.U. Jeong, J. Kang, V. Kasparcova, L.K. Leister, M.K. Mahajan, G. Miller, R. Nagilla,

- M.T. Ouellette, M.A. Reilly, A.R. Rendina, E.J. Rivera, H.H. Sun, J.H. Thorpe, R.D. Totoritis, W. Wang, D. Wu, D. Zhang, J. Bertin, R.W. Marquis, Identification of a RIP1 Kinase Inhibitor Clinical Candidate (GSK3145095) for the Treatment of Pancreatic Cancer, *ACS Med Chem Lett* 2019;10: 857-862.
- [26] J. Yuan, P. Amin, D. Ofengeim, Necroptosis and RIPK1-mediated neuroinflammation in CNS diseases, *Nat Rev Neurosci* 2019;20: 19-33.
- [27] A. Mullard, Microglia-targeted candidates push the Alzheimer drug envelope, *Nat Rev Drug Discov* 2018;17: 303-305.
- [28] D.J. Newman, G.M. Cragg, Natural products as sources of new drugs from 1981 to 2014, *J Nat Prod* 2016;79: 629-661.
- [29] D. Li, C. Li, L. Li, S. Chen, L. Wang, Q. Li, X. Wang, X. Lei, Z. Shen, Natural product Kongensin A is a non-canonical HSP90 inhibitor that blocks RIP3-dependent necroptosis, *Cell Chem Biol* 2016;23: 257-266.
- [30] C. Delehouze, S. Leverrier-Penna, F. Le Cann, A. Comte, M. Jacquard-Fevai, O. Delalande, N. Desban, B. Baratte, I. Gallais, F. Faurez, M.C. Bonnet, M. Hauteville, P.G. Goekjian, R. Thuillier, F. Favreau, P. Vandenabeele, T. Hauet, M.T. Dimanche-Boitrel, S. Bach, 6E11, a highly selective inhibitor of receptor-interacting protein kinase 1, protects cells against cold hypoxia-reoxygenation injury, *Sci Rep* 2017;7: 12931.
- [31] W.W. Chen, H. Yu, H.B. Fan, C.C. Zhang, M. Zhang, C. Zhang, Y. Cheng, J. Kong, C.F. Liu, D. Geng, X. Xu, RIP1 mediates the protection of geldanamycin on neuronal injury induced by oxygen-glucose deprivation combined with zVAD in primary cortical neurons, *J Neurochem* 2012;120: 70-77.
- [32] H. Zhang, L. Xu, X. Qin, X. Chen, H. Cong, L. Hu, L. Chen, Z. Miao, W. Zhang, Z. Cai, C. Zhuang, N-(7-Cyano-6-(4-fluoro-3-(2-(3-(trifluoromethyl)phenyl)acetamido)phenoxy)benzo[d] thiazol-2-yl)cyclopropanecarboxamide (TAK-632) Analogues as Novel Necroptosis Inhibitors by Targeting Receptor-Interacting Protein Kinase 3 (RIPK3): Synthesis, Structure-Activity Relationships, and in Vivo Efficacy, *J Med Chem* 2019;62: 6665-6681.

- [33] X. Chen, C. Zhuang, Y. Ren, H. Zhang, X. Qin, L. Hu, J. Fu, Z. Miao, Y. Chai, Z.G. Liu, H. Zhang, Z. Cai, H.Y. Wang, Identification of the Raf kinase inhibitor TAK-632 and its analogues as potent inhibitors of necroptosis by targeting RIPK1 and RIPK3, *Br J Pharmacol* 2019;176: 2095-2108.
- [34] A. Fauster, M. Rebsamen, K.V. Huber, J.W. Bigenzahn, A. Stukalov, C.H. Lardeau, S. Scorzoni, M. Bruckner, M. Gridling, K. Parapatics, J. Colinge, K.L. Bennett, S. Kubicek, S. Krautwald, A. Linkermann, G. Superti-Furga, A cellular screen identifies ponatinib and pazopanib as inhibitors of necroptosis, *Cell Death Dis* 2015;6: e1767.
- [35] M. Najjar, C. Suebsuwong, S.S. Ray, R.J. Thapa, J.L. Maki, S. Nogusa, S. Shah, D. Saleh, P.J. Gough, J. Bertin, J. Yuan, S. Balachandran, G.D. Cuny, A. Degterev, Structure guided design of potent and selective ponatinib-based hybrid inhibitors for RIPK1, *Cell Rep* 2015;10: 1850-1860.
- [36] X.Y. Wang, X.H. Zhang, L. Peng, Z. Liu, Y.X. Yang, Z.X. He, H.W. Dang, S.F. Zhou, Bardoxolone methyl (CDDO-Me or RTA402) induces cell cycle arrest, apoptosis and autophagy via PI3K/Akt/mTOR and p38 MAPK/Erk1/2 signaling pathways in K562 cells, *Am J Transl Res* 2017;9: 4652-4672.
- [37] D. Qin, W. Wang, H. Lei, H. Luo, H. Cai, C. Tang, Y. Wu, Y. Wang, J. Jin, W. Xiao, T. Wang, C. Ma, H. Xu, J. Zhang, F. Gao, Y.L. Wu, CDDO-Me reveals USP7 as a novel target in ovarian cancer cells, *Oncotarget* 2016;7: 77096-77109.
- [38] K.T. Liby, M.B. Sporn, Synthetic oleanane triterpenoids: multifunctional drugs with a broad range of applications for prevention and treatment of chronic disease, *Pharmacol Rev* 2012;64: 972-1003.
- [39] L. Avila-Carrasco, P. Majano, J.A. Sanchez-Tomero, R. Selgas, M. Lopez-Cabrera, A. Aguilera, G. Gonzalez Mateo, Natural Plants Compounds as Modulators of Epithelial-to-Mesenchymal Transition, *Front Pharmacol* 2019;10: 715.
- [40] C. Zhuang, Z. Wu, C. Xing, Z. Miao, Small molecules inhibiting Keap1-Nrf2 protein-protein interactions: a novel approach to activate Nrf2 function, *Medchemcomm* 2017;8: 286-294.
- [41] Z. Wu, Y. Geng, X. Lu, Y. Shi, G. Wu, M. Zhang, B. Shan, H. Pan, J. Yuan, Chaperone-mediated autophagy is involved in the execution of ferroptosis, *Proc Natl Acad Sci U S A* 2019;116: 2996-3005.

- [42] S.Y. Park, J.H. Shim, J.I. Chae, Y.S. Cho, Heat shock protein 90 inhibitor regulates necroptotic cell death via down-regulation of receptor interacting proteins, *Pharmazie* 2015;70: 193-198.
- [43] T. Vanden Berghe, M. Kalai, G. van Loo, W. Declercq, P. Vandenabeele, Disruption of HSP90 function reverts tumor necrosis factor-induced necrosis to apoptosis, *J Biol Chem* 2003;278: 5622-5629.
- [44] A.J. Woodhead, H. Angove, M.G. Carr, G. Chessari, M. Congreve, J.E. Coyle, J. Cosme, B. Graham, P.J. Day, R. Downham, L. Fazal, R. Feltell, E. Figueroa, M. Frederickson, J. Lewis, R. McMenamin, C.W. Murray, M.A. O'Brien, L. Parra, S. Patel, T. Phillips, D.C. Rees, S. Rich, D.M. Smith, G. Trewartha, M. Vinkovic, B. Williams, A.J. Woolford, Discovery of (2,4-dihydroxy-5-isopropylphenyl)-[5-(4-methylpiperazin-1-ylmethyl)-1,3-dihydrois oindol-2-yl]methanone (AT13387), a novel inhibitor of the molecular chaperone Hsp90 by fragment based drug design, *J Med Chem* 2010;53: 5956-5969.
- [45] A. Enomoto, T. Fukasawa, N. Takamatsu, M. Ito, A. Morita, Y. Hosoi, K. Miyagawa, The HSP90 inhibitor 17-allylamino-17-demethoxygeldanamycin modulates radiosensitivity by downregulating serine/threonine kinase 38 via Sp1 inhibition, *Eur J Cancer* 2013;49: 3547-3558.
- [46] M. Taipale, D.F. Jarosz, S. Lindquist, HSP90 at the hub of protein homeostasis: emerging mechanistic insights, *Nat Rev Mol Cell Biol* 2010;11: 515-528.
- [47] A. Degterev, D. Ofengeim, J. Yuan, Targeting RIPK1 for the treatment of human diseases, *Proc Natl Acad Sci U S A* 2019;116: 9714-9722.
- [48] B. Shan, H. Pan, A. Najafov, J. Yuan, Necroptosis in development and diseases, *Genes Dev* 2018;32: 327-340.
- [49] C. Zhuang, Z. Wang, W. Zhang, H. Ma, J. Huang, Triterpenoid derivatives as programmed cell necrosis inhibitors and their preparation, pharmaceutical compositions and use in the treatment of ischemic diseases., in: Naval Medical University (CN202010542966.3), China, 2020.
- [50] B.J. Daou, S. Koduri, B.G. Thompson, N. Chaudhary, A.S. Pandey, Clinical and experimental aspects of aneurysmal subarachnoid hemorrhage, *CNS Neurosci Ther* 2019;25: 1096-1112.

[51] O.M. Toth, A. Menyhart, V.E. Varga, D. Hantosi, O. Ivankovits-Kiss, D.P. Varga, I. Szabo, L. Janovak, I. Dekany, E. Farkas, F. Bari, Chitosan nanoparticles release nimodipine in response to tissue acidosis to attenuate spreading depolarization evoked during forebrain ischemia, *Neuropharmacology* 2020;162: 107850.

[52] J.B. Bederson, L.H. Pitts, M. Tsuji, M.C. Nishimura, R.L. Davis, H. Bartkowski, Rat middle cerebral artery occlusion: evaluation of the model and development of a neurologic examination, *Stroke* 1986;17: 472-476.

Journal Pre-proof

1. Bardoxolone (CDDO) was identified as a necroptosis inhibitor.
2. Further optimization led to identify a more potent analogue 20.
3. It blocked necrosome formation by targeting Hsp90 to inhibit the phosphorylation of RIPK1 and RIPK3 in necroptotic cells.
4. In vivo, this compound was orally active to alleviate TNF-induced systemic inflammatory response syndrome (SIRS) and cerebral I/R injury.

Journal Pre-proof

Declaration of interests

The authors declare that they have no known competing financial interests or personal relationships that could have appeared to influence the work reported in this paper.

The authors declare the following financial interests/personal relationships which may be considered as potential competing interests:

Journal Pre-proof